HOKKAIDO UNIVERSITY

Title	Relationships between dissolved black carbon and dissolved organic matter in streams
Author(s)	Yamashita, Youhei; Kojima, Daiki; Yoshida, Natsumi; Shibata, Hideaki
Citation	Chemosphere, 271, 129824 https://doi.org/10.1016/j.chemosphere.2021.129824
Issue Date	2021-05
Doc URL	http://hdl.handle.net/2115/89114
Rights	© 2021. This manuscript version is made available under the CC-BY-NC-ND 4.0 license https://creativecommons.org/licenses/by-nc-nd/4.0/
Rights(URL)	http://creativecommons.org/licenses/by-nc-nd/4.0/
Type	article (author version)
File Information	CHEM80156.pdf

Relationships between dissolved black carbon and dissolved organic matter in streams

Youhei Yamashita[1,2,*], Daiki Kojima[2], Natsumi Yoshida[2], Hideaki Shibata[2,3]

[1] *Faculty of Environmental Earth Science, Hokkaido University, Sapporo, Japan*
[2] *Graduate School of Environmental Science, Hokkaido University, Sapporo, Japan*
[3] *Field Science Center for Northern Biosphere, Hokkaido University*

*yamashiy@ees.hokudai.ac.jp

Highlights

・Stream DBC, in which the catchment was unaffected by fire, was studied

・Atmospheric deposition of BC to the catchment is predominant source of stream DBC

・DBC concentration was linearly correlated with DOC concentration

・The degree of DBC polycondensation was correlated with bulk DOC quality

・Mobilization mechanism from soil to stream was similar between DBC and DOC
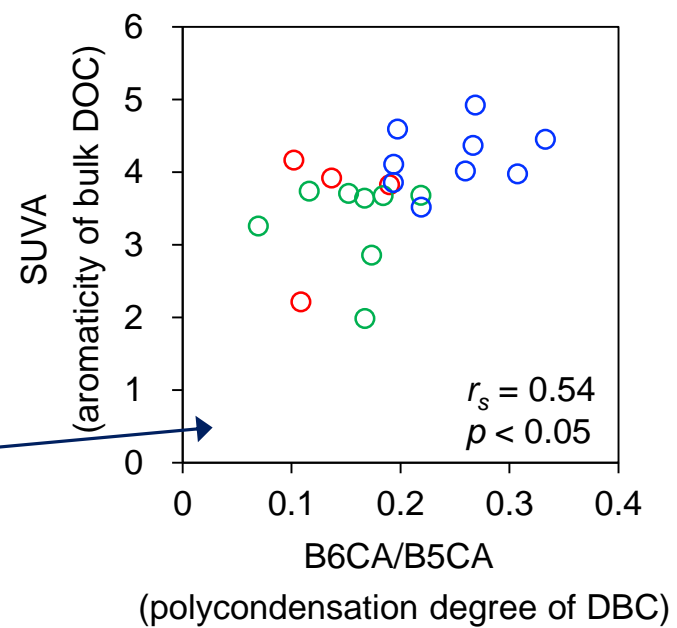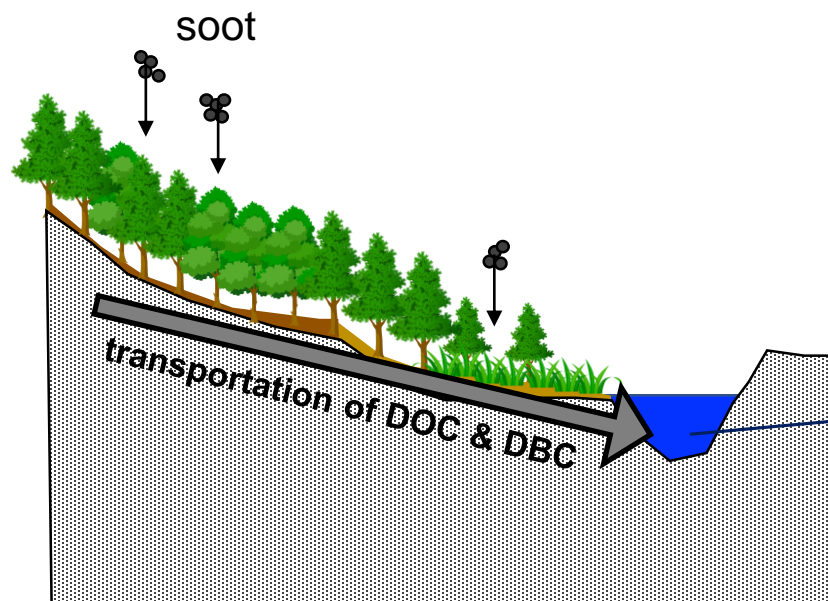
Abstract

Black carbon (BC) is a pyrolyzed product derived from incomplete combustion. A major

fraction of BC produced by landscape fires is initially deposited onto onsite soils.

Atmospheric deposition of soot is known to be an important source of soil BC, especially in

watersheds that are not affected by landscape fires. The transport of the dissolved fraction

of oxidized BC in soil, defined as dissolved black carbon (DBC), to streams is considered

one of the important loss pathways of BC in soil, but the mechanism is not well

documented. We measured the quantity and quality of DBC, determined by a

benzenepolycarboxylic acid method, and the quantitative and qualitative parameters of bulk

dissolved organic matter (DOM) in streams in Hokkaido, northern Japan, whose

catchments were not affected by landscape fire for at least 110 years. DBC with relatively

low polycondensed signatures occurred in the streams, irrespective of differences in

watershed characteristics and seasons, suggesting that atmospheric deposition of soot into

the catchment is probably a major source of stream DBC. The DBC concentration was

linearly related to the dissolved organic carbon (DOC) concentration, irrespective of the

differences in watershed characteristics and seasons. Furthermore, the polycondensation

degree of DBC was observed to correlate with the qualitative parameters of bulk DOM.

Such quantitative and qualitative relationships between DBC and bulk DOM imply that the

transfer mechanism from soils to streams of soot-derived polycondensed DBC is linked

with that of higher plant-derived, high-molecular-weight aromatic DOM.

36   **Keywords**

37   dissolved black carbon; dissolved organic matter; streams; soot; mobilization

38

1. Introduction

Black carbon (BC) is a pyrolyzed product derived from incomplete combustion during biomass burning as well as fossil fuel combustion and includes soot, charcoal, and slightly charred biomass (Masiello, 2004). BC is chemically heterogeneous but has a high carbon content and condensed aromatic structures (Hedges et al., 2000; Masiello, 2004; Wonizak et al., 2020). Although BC produced under low charring temperatures, e.g., levoglucosan, is highly water soluble and biodegradable (Myers-Pigg et al., 2015), the major fraction of BC with polycyclic aromatic structures is considered to be resistant to biodegradation for at least thousands of years (Masiello and Druffel, 1998). The majority of biomass is completely oxidized to CO_2 during a landscape fire, including wildfires, deforestation fires and agricultural burns, while 5–15% of the biomass is converted to BC (Santín et al., 2016). A recent study estimated that 2.2 PgC of CO_2 is emitted into the atmosphere, and 0.26 PgC of biomass carbon is converted to BC by annual landscape fires (Jones et al., 2019a). In addition, 0.002–0.029 PgC yr^{-1} of BC was estimated to be emitted into the atmosphere globally by fossil fuel combustion and biomass burning (Bond et al., 2013). This BC is eventually deposited on the land or ocean and impacts biogeochemical cycles as well as ecosystems (Mari et al., 2014; 2019).

A part of BC produced during landscape fires is emitted to the atmosphere mainly as soot, but the major fraction of BC is initially deposited onto onsite soils mainly as charcoal (Kuhlbusch, 1998; Santín et al., 2016). Otherwise, BC is redistributed to stream corridors or transported to rivers as particulate BC with overland flow (Wagner et al., 2015; Cotrufo et al., 2016). The riverine flux of particulate BC is found to be primarily controlled by erosion (Wagner et al., 2015; Cotrufo et al., 2016, Coppola et al., 2018). The annual global

4

62 flux of riverine particulate BC to the ocean was estimated to be 0.017 to 0.037 PgC

63 (Coppola et al., 2018), which is equivalent to 6.5 to 14.2% of 0.26 PgC, the annually

64 produced BC by landscape fires (Jones et al., 2019a).

65   As BC incorporated in soils ages, BC becomes water soluble due to the introduction of

66 oxygen- and nitrogen-containing functionalities (Knicker, 2011). The soluble fraction of

67 BC in soil pore water is known to be exported to rivers (Hockaday et al., 2006; 2007). The

68 long-term effects of slash and burn activities on the riverine export of dissolved BC (DBC,

69 having condensed aromatic structures, detected by a benzenepolycarboxylic acid (BPCA)

70 method), have been demonstrated (Dittmar et al., 2012). On the other hand, it has been

71 pointed out that anthropogenic BC, associated with soot, is the most prominent source of

72 DBC in glacial rivers (Stubbins et al., 2012; Ding et al., 2015). It has also been documented

73 that BC atmospherically deposited onto vegetation is transferred to soil by throughflow and

74 stemflow (Stubbins et al., 2017; Wagner et al., 2019b), and soot-derived BC deposited in

75 watersheds is reported to be exported to rivers as DBC (Wang et al., 2016; Jones et al.,

76 2017; 2019b). The relationships between riverine DBC parameters and land use variables

77 showed that riverine DBC is generally less polycondensed in anthropogenically disturbed

78 areas of the watershed, namely, urban and agricultural areas (Roebuck et al., 2018a). It was

79 estimated that 0.027 PgC of DBC is transported annually to the global ocean (Jaffé et al.,

80 2013). The flux has been updated to 0.018 PgC yr^{-1} (Jones et al., 2020). The riverine DBC

81 flux is ~10% of the annual BC production by landscape fires (Jones et al., 2019a) and is

82 one order of magnitude larger than the annual atmospheric deposition of BC to the ocean

83 (~0.002 PgC) (Santín et al., 2016); therefore, the transport of DBC from the soil to rivers is

84 a key factor shaping the distributional pattern of BC on the Earth's surface. However, it

85   should be noted that a recent study, which determined the $\delta^{13}C$ of riverine and oceanic

86   BPCA, revealed that oceanic DBC does not predominantly originate from rivers (Wagner et

87   al., 2019a).

88   Recent studies have reported the coupling of the spatial distribution of dissolved

89   organic carbon (DOC) and DBC in fluvial systems with global (Jaffé et al., 2013), regional

90   (Ding et al., 2015; Stubbins et al., 2015) and different catchment scales (Ding et al., 2013;

91   2014; Güereña et al., 2015). Jaffé et al. (2013) suggested that the coupling of DOC and

92   DBC is possibly due to the same diagenetic processes driving the release of DOC and DBC

93   from soils or the ability of DOC as a mobilizing agent of DBC through hydrophobic

94   interactions. On the other hand, decoupling of DOC and DBC was observed for temporal

95   variations in both parameters for streams and large rivers (Wang et al., 2016; Roebuck et

96   al., 2018b; Bao et al., 2019). Such decoupling of the two parameters was explained by

97   different source contributions, in particular anthropogenic sources (Wang et al., 2016;

98   Roebuck et al., 2018b), or by the delayed recovery of soil pore water DBC stocks relative

99   to pore water DOC stocks following rainfall (Jones et al., 2019b). As such, factors

100   controlling DBC export from soil to rivers have not been well constrained (Wagner et al.,

101   2018).

102   This study measured DBC in streams with different types of watershed characteristics

103   in a transitional area from a cool-temperate zone to a boreal zone in Hokkaido, northern

104   Japan. An important aspect of the watershed compared with other studies is fire history.

105   The watershed was not affected by landscape fire for at least 110 years, and therefore, a

106   major source of stream DBC is probably soot deposited in the catchment rather than

107   charcoal produced by landscape fire. The bulk dissolved organic matter (DOM) parameters

108 and their optical proxies were analyzed together with DBC quality and quantity determined

109 using the BPCA method. The main purpose of this study was to assess the DBC export

110 from the soil to the stream in a watershed not affected by landscape fires for the last 110

111 years. To achieve this purpose, we evaluated the quantitative and qualitative relationships

112 between the parameters DBC and bulk DOM and clarified the linkage between the

113 transport mechanisms of DBC and bulk DOM.

114

115 **2. Materials and methods**

116 **2.1. Study site**

117   The studied streams are located in Hokkaido University's Uryu Experimental Forest

118 (UREF), northern Hokkaido, Japan (Fig. 1). UREF is a part of the North Hokkaido

119 Experimental Forest, a core site of the Japan Long Term Ecological Research Network

120 (JaLTER). The climate is characterized by cold temperatures (minimum temperature is ca. -

121 35°C) and heavy snowfall (200 cm or greater of maximum snowpack depth) in winter with

122 a 4.2°C mean annual air temperature and 1467 mm mean annual precipitation (Ozawa et

123 al., 2001). Stream discharge reaches its maximum during spring snowmelt (Ogawa et al.,

124 2006), and the plant-growing season is restricted to a short summer (June to September)

125 (Seki et al., 2010). Vegetation in the forest area is characterized by a cool-temperate mixed

126 forest composed of natural broad-leaved deciduous hardwood and evergreen coniferous

127 species with dense Sasa dwarf bamboo as understory vegetation (Ogawa et al., 2006; Seki

128 et al., 2010). Stream water samples were collected from the Dorokawa River (D),

129 Butokamabetsu River (B), and Akaishi River (A) in the UREF (Fig. 1). The watersheds of

130 the Dorokawa and Butokamabetsu Rivers are almost all natural forest areas, but that of the

131   Akaishi River is partly in pastureland for dairy cattle farming (Hino et al., 2006). The

132   upstream Dorokawa River is covered by natural forest, while there are several types of

133   wetlands, i.e., spruce-swamp forests, open mire, and riparian wetlands, downstream

134   (Ogawa et al., 2006).

135   There has been no record of landscape fire around the studied watershed since the

136   establishment of the UREF in 1901. The UREF is located approximately 70 km and 160

137   km north of Asahikawa (population, 0.4 million) and Sapporo (population, 2 million),

138   respectively (Fig. 1). Hokkaido is known to be affected by the long-range transport of BC

139   from eastern Eurasia to the outflow region (Zhu et al., 2019). Therefore, atmospheric

140   deposition of soot produced by fossil fuel combustion and biomass burning in Hokkaido

141   and/or eastern Eurasia are probable major sources of BC in the UREF.

142

143   **2.2. Field observations and sampling**

144   Stream water samples for DBC analysis were collected from sites D, B, and A on 10

145   June 2011, 24 October 2011, 24 January 2012, 17 April 2012, and 10 September 2012.

146   Additionally, water samples were collected from tributaries of the Dorokawa River, whose

147   watersheds were covered by forest (DF) and wetlands (DW) (Fig. 1), on 24 October 2011,

148   24 January 2012, 17 April 2012, and 10 September 2012. Approximately 10 L of water was

149   collected in an acid-cleaned tank. Just after sampling, a water sample was transferred to the

150   laboratory and filtered through a precombusted (450°C, 3 h) Whatman GF/F filter (0.7 μm

151   nominal pore size), and the pH of the filtrate was adjusted to 2 with HCl. The acidified

152   filtrate was then immediately subjected to solid-phase extraction (SPE) (1 g, Bond Elut

153   PPL, Agilent Technologies). The SPE cartridge was immediately dried under a N_2 stream,

154   and the organic matter adsorbed on the SPE resin was eluted by methanol, according to

155   Dittmar et al. (2008). The eluate was poured into a glass vial with a Teflon-lined cap and

156   then stored in the dark in a freezer.

157   The separate water sample was also collected in an acid-cleaned 250 ml polypropylene

158   bottle for bulk DOM analysis. The sample was filtered using a precombusted Whatman

159   GF/F filter. The pH of filtrate was not changed. DOC concentration, fluorescence spectrum,

160   and absorbance spectrum were measured just after filtration, while samples for total

161   dissolved nitrogen (TDN) and nutrient ($NO_3^-+NO_2^-$, and NH_4^+) analyses were stored in the

162   dark in a freezer. Samples for bulk DOM analysis were generally collected biweekly from

163   June 2011 to October 2012, and then, DOC concentrations were determined.

164   Precipitation data observed at the headquarter office of UREF were obtained from the

165   JaLTER Database (http://db.cger.nies.go.jp/JaLTER/, Metadata ID: JaLTER-Hokkaido-

166   Kita.16.9). Stream discharge was calculated from the recorded water level and the H-Q

167   curve obtained at site D of the Dorokawa River and site B of the Butokamabetus River

168   (Ogawa et al., 2006). Stream discharge was not determined during winter due to river

169   freezing.

170

171   **2.3. Chemical analysis**

172   DBC analysis was performed by the BPCA method according to Dittmar (2008) with

173   some modifications. In 2020, the methanol eluate that had been stored in a freezer in the

174   dark, corresponding to 0.3 to 1.5 L of original water, was transferred into 2 mL glass

175   ampoules and dried on a centrifugal vacuum evaporator (CVE-3000, EYELA) at 50°C.

176   Then, 0.5 mL of concentrated HNO_3 was added to the ampoule, and the ampoule was

9

177   flame-sealed and kept in an oven at 170°C for 6 h according to Nakane et al. (2017). After

178   oxidation, HNO_3 was evaporated to dryness in a centrifugal vacuum evaporator at 50°C.

179   The oxidation residue in the ampoules was redissolved in 0.2 mL of mobile phase A (4 mM

180   tetrabutylammonium bromide, 50 mM sodium acetate, and 10% MeOH) to quantify

181   BPCAs, namely, benzenepentacarboxylic acid (B5CA) and benzenehexacarboxylic acid

182   (B6CA), using high-performance liquid chromatography (HPLC) with a photodiode array

183   detector (1260 Infinity, Agilent). Analytical conditions of reverse-phase HPLC with mobile

184   phases A and B (MeOH) were based on Dittmar (2008). Benzenetricarboxylic acids

185   (B3CA) and benzenetetracarboxylic acids (B4CA) were not determined in this study

186   because these compounds were shown to be produced from molecules with no condensed

187   aromatic functionalities, such as lignin (Kappenberg et al., 2016; Bostick et al., 2018).

188   The DBC concentration was estimated from the BPCA concentrations using equation

189   (1) based on Stubbins et al. (2015).

190       $[DBC] = 12.01 \times 0.0891 \times ([B6CA + B5CA])^{0.9175}$ (1)

191   The units of [DBC] and [BPCAs] were $\mu gC\ L^{-1}$ and nM, respectively. The molar ratio of

192   B6CA to B5CA (B6CA/B5CA) was calculated as the polycondensation degree of DBC

193   (Stubbins et al., 2015; Marques et al., 2017). The analytical error determined with replicate

194   analyses (n=4) of a sample from a stream in the UREF was 5.0% and 4.1% for the DBC

195   concentration and the B6CA/B5CA ratio, respectively.

196   The DOC concentration was determined by a high-temperature catalytic oxidation

197   method (TOC-V$_{CSH}$, Shimadzu). A standard curve with a series of glucose solutions

198   determined daily was used for calibration.

10

199   Absorbance analysis of DOM was carried out using a spectrophotometer (UV-1800,

200   Shimadzu) with a 1 cm cuvette. The absorbance spectrum was determined from 250 to 800

201   nm at 0.5 nm intervals under a medium scan speed. The absorbance spectrum of the sample

202   was baseline-corrected by subtracting average values ranging from 700 to 800 nm from the

203   entire spectrum. The Napierian absorption coefficient at 254 nm, a_{254} (m^{-1}), was reported as

204   a quantitative parameter of chromophoric DOM (CDOM). Specific UV absorbance

205   (SUVA) was calculated by dividing the Decadic absorbance at 254 nm, A_{254} (m^{-1}), by the

206   DOC concentration (mg L^{-1}) (Weishaar et al., 2003). The S_R value, the ratio of the spectral

207   slope parameter (S) obtained from the two regions, 275 to 295 nm ($S_{275-295}$) and 350 to 400

208   nm ($S_{350-400}$), was calculated according to Helms et al. (2008).

209   Excitation-emission matrix (EEM) fluorescence was determined with a fluorometer

210   (FluoroMax-4, Horiba) according to Tanaka et al. (2014) with some modifications. Forty-

211   one emission scans from 290 to 550 nm taken at 2-nm intervals were acquired for

212   excitation wavelengths between 250 and 450 nm at 5-nm intervals. The bandpass was set to

213   5 nm for both excitation and emission monochromators, and the integration time was set to

214   0.1 seconds. The fluorescence spectra were acquired in S/R mode. Several postacquisition

215   steps were involved in the correction of the fluorescence spectrum, including inner filter

216   correction with absorbance spectrum, instrumental bias correction, and the subtraction of

217   the EEM of Milli-Q water (Murphy et al., 2010). The fluorescence unit was converted to a

218   Raman unit (RU) with a water Raman peak (excitation=350 nm) of Milli-Q water analyzed

219   daily (Lawaetz and Stedmon, 2009). The fluorescence index was calculated as the ratio of

220   fluorescence intensities at 470 nm and 520 nm emissions at 370 nm excitation according to

221   Cory and McKnight (2005). Parallel factor analysis (PARAFAC) was conducted in

222   MATLAB (Mathworks, Natick, MA) using the DOMFluor toolbox (Stedmon and Bro,

223   2008) with 205 EEMs collected from streams in the UREF watersheds. A four-component

224   model was validated according to Stedmon and Bro (2008). Following Coble (2007), C1,

225   C2, and C3 (Fig. S1) were assigned as humic-like components, and C4 (Fig. S1) was

226   identified as a protein-like component.

227   TDN and nutrient ($NO_3^-+NO_2^-$, and NH_4^+) concentrations were determined using a

228   continuous flow analyzer (Hansen and Koroleff, 1999) with a built-in wet oxidation system

229   by potassium persulfate (QuAAtro, Bran+Luebbe Analytics). The dissolved organic

230   nitrogen (DON) concentration was determined by subtracting the inorganic nutrient

231   concentrations from the TDN concentration. The C/N ratio of bulk DOM was calculated as

232   the molar ratio of DOC concentration to DON concentration.

233

234   **2.4. Statistical analysis**

235   The differences in DBC parameters, i.e., the DBC contribution of DOC (DBC/DOC, %)

236   and the B6CA/B5CA ratio, among watersheds were examined. The Shapiro-Wilk test

237   indicated that the DBC parameters in the three watersheds followed a normal distribution

238   (Table S1). However, due to the small number of samples, we used a nonparametric

239   Wilcoxon rank sum test as well as a parametric t-test for the comparison of DBC

240   parameters. Spearman's rank correlation coefficient and Kendall's rank correlation

241   coefficient were determined between DBC and the bulk DOM parameters. The results of

242   Kendall's rank correlation test can be found in Supplementary Tables and Figures.

243   Spearman's rank correlation coefficient and Kendall's rank correlation coefficient were also

244   determined for DBC and DOC *vs.* discharge and precipitation. The precipitation data

245 obtained from April to October were used for the correlation analyses to eliminate snowfall.

246 Since many values of precipitation were 0 during the observation of DOC, correlation

247 coefficients were not determined between DOC and precipitation. A confidence level (α) of

248 95% was used for all statistics. The Wilcoxon rank sum test, t-test, Spearman's rank

249 correlation test, and Kendall's rank correlation test were carried out with R (version 3.5.1).

250

251 **3. Results**

252 **3.1. Temporal variability of DOC and DBC in streams**

253   Figure 2 shows temporal variations in the DOC concentration, DBC concentration, and

254 B6CA/B5CA ratio value at sites D, B, and A with precipitation and stream discharge. The

255 DOC concentration at site D, which was partly covered by wetlands, ranged from 1.0 to 5.4

256 mgC L^{-1} (Fig. S2). The concentrations were generally higher than those at site B (0.5–4.8

257 mgC L^{-1}), where the watershed was covered by natural forest, and site A (0.8–7.1 mgC L^{-1}),

258 where the watershed was used for pastureland (Fig. S2). The DOC concentrations at site A

259 tended to be slightly higher than those at site B. Temporal variations in the DOC

260 concentration were similar among the three sites. Stream discharge showed a broad

261 maximum with some spikes in the spring due to snowmelt. The DOC concentration was not

262 high during snowmelt (Fig. 2) and was not significantly correlated with stream discharge

263 (p=0.18, n=25 for site D; p=0.70, n=25 for site B; Spearman's rank correlation; Fig. S3).

264 Peaks of the DOC concentration were observed on 15 August 2011 and 10 September

265 2012. Both peaks corresponded to small peaks of stream discharge with precipitation (Fig.

266 2 and Fig. S3).

267   The DBC concentrations at the three sites were highest on 10 September 2012 when the

268   DOC concentrations peaked (Fig. 2). The DBC concentrations at site D (0.052–0.304 mgC

269   L^{-1}) were always higher than those at sites B (0.026–0.166 mgC L^{-1}) and A (0.033–0.129

270   mgC L^{-1}), while the concentrations were similar between sites B and A throughout the

271   observations (Fig. S4). The DBC concentration was not significantly correlated with stream

272   discharge (p=0.42, n=4 for site D; p=0.92, n=4 for site B, Spearman's rank correlation; Fig.

273   S5) or precipitation (p=0.33, n=4 for site D; p=0.75, n=4 for site B; p=0.33, n=3 for site A;

274   Spearman's rank correlation; Fig. S6). The B6CA/B5CA ratio values ranged from 0.19 to

275   0.31, from 0.10 to 0.19, and from 0.12 to 0.22 at sites D, B, and A, respectively (Fig. 2 and

276   Fig. S4). The B6CA/B5CA ratio value was always highest at site D and lowest at site A,

277   except on 24 October 2011. The ratios at the three sites did not show a clear trend on 10

278   September 2012 when the DBC concentration was highest, even though the ratios at sites B

279   and A on that observation day were highest. The ratio was not significantly correlated with

280   stream discharge (p=0.92, n=4 for site D; p=0.75, n=4 for site B; Spearman's rank

281   correlation; Fig. S5) or precipitation (p=0.75, n=4 for site D; p=0.33, n=4 for site B; p=1,

282   n=3 for site A; Spearman's rank correlation; Fig. S6).

283   Figure 3 shows the relationships between the DBC concentration and DOC

284   concentration as well as a_{254} for all samples collected from all sites (i.e., sites D, B, A, DF,

285   and DW). The DBC and DOC concentrations were linearly correlated for all samples

286   ([DBC] = 0.054×[DOC] – 0.022, r^2=0.95, p<0.01, n=21). On the other hand, DBC/DOC

287   (%) was significantly different between the wetland area (4.8±0.7% for D and DW) and

288   forest area (4.3±0.5% for B and DF) and pastureland area (3.5±0.9% for A) (p<0.05 for t-

289   test and Wilcoxon rank sum test; Table S2 and Fig. S7). The contribution was not

14

290   significantly different between the forest area and pastureland area (p=0.49 and 0.57 for t-

291   test and Wilcoxon rank sum test, respectively; Table S2 and Fig. S7). The DBC

292   concentration was also linearly correlated with a_{254} ([DBC] = $0.0053 \times [a_{254}] - 0.0065$,

293   r^2=0.97, p<0.01, n=21) and with humic-like components (p<0.01) but not with a protein-

294   like component (p=0.08) obtained by EEM-PARAFAC (Fig. S8).

295

296   **3.2. Relationships among qualitative parameters of DBC and bulk DOM**

297   The polycondensation degree of DBC, as determined by the B6CA/B5CA ratio, was

298   significantly different between the wetland area (0.25±0.05 for D and DW) and forest area

299   (0.16±0.05 for B and DF) and pastureland area (0.13±0.04 for A) (p<0.01 for t-test and

300   Wilcoxon rank sum test; Table S2 and Fig. S7). The ratio was not significantly different

301   between the forest area and pastureland area (p=0.43 and 0.46 for t-test, respectively; Table

302   S2 and Fig. S7).

303   The relationships among the qualitative parameters of DBC and bulk DOM were

304   determined for all samples collected from all sites (Fig. 4, Table S3, and Fig. S9).

305   DBC/DOC (%) was significantly positively correlated with SUVA, i.e., the ratio of CDOM

306   to DOC (r_s=0.74, p<0.01, n=21, Spearman's rank correlation). A significant positive

307   correlation was also evident between DBC/DOC and B6CA/B5CA (r_s=0.67, p<0.01, n=21,

308   Spearman's rank correlation). DBC/DOC was also significantly correlated with S_R (r_s=-

309   0.66, p<0.01, n=21, Spearman's rank correlation) and the C/N of bulk DOM (r_s=0.53,

310   p<0.05, n=21, Spearman's rank correlation) but not with the fluorescence index (p=0.07,

311   n=21, Spearman's rank correlation) (Fig. S9). The B6CA/B5CA ratio value was

312   significantly positively correlated with the C/N of bulk DOM (r_s=0.60, p<0.01, n=21,

15

313 Spearman's rank correlation) and SUVA (r_s=0.54, $p<0.05$, n=21, Spearman's rank

314 correlation) but was negatively correlated with S_R (r_s=-0.51, $p<0.05$, n=21, Spearman's rank

315 correlation) and fluorescence index (r_s=-0.66, $p<0.01$, n=21, Spearman's rank correlation).

316 The B6CA/B5CA ratio value was also significantly correlated with the DBC concentration

317 (r_s=0.68, $p<0.01$, n=21, Spearman's rank correlation), DOC concentration (r_s=0.66, $p<0.01$,

318 n=21, Spearman's rank correlation), and a_{254} (r_s=0.69, $p<0.01$, n=21, Spearman's rank

319 correlation) (Fig. S9).

320

321 **4. Discussion**

322 **4.1. Stream DBC characteristics and its origin**

323 The DBC contribution to the DOC (%) ranged from 3.5±0.9% for pastureland to

324 4.8±0.7% for wetlands in streams of the UREF watersheds and was smaller than the

325 10.6±0.7% global average (Jaffé et al., 2013). DBC contributions have recently been

326 determined to significantly differ among biomes (Jones et al., 2020), and the contributions

327 observed in streams in the UREF watersheds were similar to those in temperate forests

328 (4.4±2.5%) and boreal forests (5.4±1.1%) (Jones et al., 2020).

329 It has been documented that DBC is produced from not only fresh charcoal but also old

330 charcoal (Abiven et al., 2011; Wagner et al., 2017), and DBC has been continuously

331 released into rivers for a long time through the degradation of historically accumulated soil

332 BC (Dittmar et al., 2012; Marques et al., 2017). It is possible that an ancient forest fire

333 event contributed to the DBC in the studied streams, even though the sites were unburned

334 for at least 110 years.

335   Recent studies have indicated that atmospheric deposition of BC to watersheds is a

336   source of DBC in soil water (Santos et al., 2017) as well as riverine DBC (Jones et al.,

337   2017; 2019b). It has also been documented that BC atmospherically deposited onto

338   vegetation is transferred to riverine catchments by throughflow and stemflow (Stubbins et

339   al., 2017; Wagner et al., 2019b). It is interesting to note that recent studies have suggested

340   that the DBC derived from soot is less polycondensed than that from charcoal produced by

341   a wildfire (Ding et al., 2015; Roebuck et al., 2018a; Coppola et al., 2019). Ding et al.

342   (2015) reported that the DBC in the water soluble fraction extracted from atmospheric dust

343   was less polycondensed than wildfire-derived DBC, and Roebuck et al. (2018a) suggested

344   that atmospheric deposition of soot or polyaromatic hydrocarbons contributed to the less

345   polycondensed DBC signature in streams in the urban area of the Altamaha watershed. A

346   negative relationship between the polycondensation degree, namely, B6CA/B5CA, in

347   riverine DBC and the fossil fuel BC deposition rate integrated in corresponding

348   subcatchments was also found in the Amazon River (Coppola et al., 2019). The

349   B6CA/B5CA ratio of the DBC observed in streams in the UREF watersheds was generally

350   lower than that of the DBC in an area of the Amazon River subcatchment (B6CA/B5CA of

351   0.26), which is the most affected by the atmospheric deposition of BC produced by fossil

352   fuel combustion in addition to charcoal produced by landscape fires. The B6CA/B5CA

353   ratio of the DBC in streams of the UREF was also generally lower than the ratio of the

354   water-soluble fraction extracted from atmospheric dust (B6CA/B5CA of 0.32, Ding et al.,

355   2015). Additionally, the DBC concentration was not significantly correlated with

356   precipitation for the UREF watersheds (Fig. S6), implying that soot and DBC in

357   precipitation are unlikely to contribute directly to DBC in the streams. These pieces of

358 evidence suggest that atmospheric deposition of soot on the soil of the catchment and

359 subsequent mobilization and transport of soot-derived BC to the stream are probably the

360 major sources of DBC in the UREF watersheds.

361

362 **4.2. Factors controlling DBC export from soils to streams**

363 The DOC and DBC concentrations were not significantly correlated ($p>0.05$) with

364 stream discharge (Fig. 2, Figs. S3 and S5). Positive relationships between river (stream)

365 discharge and DOC concentration (e.g., Holmes et al., 2008; Wilson et al., 2013) and DBC

366 concentration (Dittmar et al., 2012; Stubbins et al., 2015; Wagner et al., 2015), indicative of

367 flushing of high levels of DOC and DBC from upper soil horizons under high flow

368 conditions, have often been observed. On the other hand, in addition to the discharge,

369 antecedent moisture conditions were determined to control the DOC concentration under

370 high flow conditions (Inamdar et al., 2008; Oswald and Branfireun, 2014). The different

371 effects of antecedent precipitation on riverine DOC and DBC concentrations due to the

372 quick and slow rebound of porewater DOC and DBC concentrations after precipitation,

373 respectively, were also noted for the Amazon River (Jones et al., 2019b). In our study, two

374 spikes of DOC concentration were found in the small peaks of discharge with precipitation

375 events after relatively long nonprecipitation periods (Fig. 2). These results suggest that

376 spikes in the DOC and DBC concentrations observed in the UREF watersheds were

377 possibly affected by antecedent precipitation. Further observations are needed to determine

378 the factors controlling temporal variations in DOC and DBC concentrations in the UREF

379 watersheds.

18

380   The DBC concentration was linearly related to the DOC concentration, irrespective of

381   differences in seasons and watershed characteristics (Fig. 3a), even though the DBC/DOC

382   (%) was different among the watersheds with different characteristics. Linear relationships

383   between the two parameters have also been observed from the watershed scale to the global

384   scale (Jaffé et al., 2013; Ding et al., 2013; 2014; 2015; Stubbins et al., 2015; Wagner et al.,

385   2015). On the other hand, decoupling of the DBC concentration and DOC concentration,

386   probably due to the different source contributions, particularly anthropogenic source

387   contributions (Wang et al., 2016; Roebuck et al., 2018b), or the divergent effects of soil

388   properties, temperature, rainfall, and aerosol deposition (Bao et al., 2019; Jones et al.,

389   2019b), has also been reported. Interestingly, it has been pointed out that charcoal in soils

390   supplies DBC to channels at baseflow, and atmospherically deposited soot contributes as an

391   additional source of riverine DBC during high-flow regimes (Roebuck et al., 2018b; Jones

392   et al., 2019b). Such a shift in DBC sources to channels was suggested to be a reason for

393   seasonal decoupling of DOC and DBC (Roebuck et al., 2018b; Jones et al., 2019b). The

394   major source of DBC in the stream in the UREF watersheds during the baseflow as well as

395   spikes of the discharge was possibly mobilization from the soot deposited on the soil in the

396   watersheds but was not direct contribution of soot and DBC in precipitation (Fig. S6).

397   Therefore, the reason for the linear relationship between the DBC and DOC concentrations

398   observed in this study might be the result of the coupled transport of soot-derived DBC and

399   DOC from the soil to the stream.

400   The DBC/DOC (%) and B6CA/B5CA ratio values in streams with wetlands in the

401   watersheds were significantly higher than those in streams in which watersheds were

402   completely covered by forests and partly covered by pastureland (Fig. S7). In addition, a

19

403 positive correlation was evident between the two parameters (Fig. 4b). A significant

404 positive correlation was also observed between DBC/DOC and B6CA/B5CA in small

405 watersheds in the southeastern part of China and was considered a result of

406 photodegradation of DBC (Bao et al., 2019). The streams observed in this study were near

407 headwater regions that are heavily forested (Fig. 1), suggesting that a process other than

408 photodegradation must be causing changes in DBC/DOC and B6CA/B5CA in this study.

409   Roebuck et al. (2018a) found that the DBC concentration and BPCA ratio in river water

410 were positively correlated with wetland coverage but were negatively correlated with urban

411 land use in the Altamaha River, a large subtropical watershed. Such relationships were

412 considered to be the result of changes in the DBC sources along the river from fire-derived

413 charcoal in wetlands to fossil fuel combustion-derived soot in urban areas (Roebuck et al.,

414 2018a). Since the major source of DBC in the UREF watersheds is probably soot deposited

415 on the soil of the watershed, the differences in the source may not solely account for the

416 differences in DBC/DOC and B6CA/B5CA among the watersheds in the UREF. Kothawala

417 et al. (2012) showed that larger aromatic compounds can be preferentially adsorbed in

418 mineral-rich soils. Thus, a fraction having relatively highly polycondensed DBC mobilized

419 from soot deposited onto soil may be preferentially retained in mineral-rich soils in forested

420 and pastureland areas, resulting in a lower polycondensation degree of riverine DBC in

421 forested and pastureland areas than in wetland areas.

422   The linear relationship between the DBC concentration and DOC concentration has

423 been interpreted as the result of similar diagenetic processes driving the release of DOC and

424 DBC from soils or intermolecular associations between DOC and DBC through

425 hydrophobic interactions (Jaffé et al., 2013). In addition to the linear relationship between

426 the two parameters, we found significant correlations between the polycondensation degree

427 of DBC (B6CA/B5CA) and the qualitative parameters of bulk DOM in the UREF

428 watersheds (Fig. 4). SUVA is positively related to the aromaticity of DOM (Weishaar et al.,

429 2003), while S_R is negatively related to the molecular weight of DOM (Helms et al., 2008).

430 Therefore, positive and negative correlations between B6CA/B5CA and SUVA and S_R,

431 respectively, indicate that the environmental dynamics of polycondensed DBC are similar

432 to those of high-molecular-weight aromatic DOM. The polycondensation degree of DBC

433 was also positively correlated with the C/N of bulk DOM but negatively correlated with the

434 fluorescence index of bulk DOM. A high value of C/N and a low value of the fluorescence

435 index indicate a higher plant origin of DOM (McKnight et al., 1997; 2001). In conclusion,

436 the qualitative relationships between DBC and DOC observed in this study indicate that the

437 transfer mechanism from soils to streams, namely, the release and subsequent adsorption

438 and desorption processes, is similar between DBC derived from soot deposited on soil and

439 higher plant-derived, high-molecular-weight aromatic DOM. This conclusion is supported

440 by the significant positive correlation between SUVA and DBC/DOC (Fig. 4a).

441   The results of controlled DBC leaching experiments using charcoal and wildfire-

442 influenced soil samples did not determine the effect of DOM as a mobilizing agent through

443 hydrophobic interactions (Wagner et al., 2017). Wagner et al. (2017) also determined the

444 octanol-water partition coefficients of modeled DBC and noted that a considerable portion

445 of the DBC pool that has been quantified in aquatic environments is not truly dissolved.

446 Knowledge of "DBC speciation" will help to better understand the biogeochemical

447 mechanisms that control the transfer of BC from soils to streams. The soot from urban dust

448 probably releases more DBC than charcoal produced from onsite soils, since the

449 polycondensation degree of DBC dissolved from soot is lower than that from charcoal

450 (Ding et al., 2015). Therefore, the soot/charcoal ratio in soils is possibly a factor that

451 controls the mobility of DBC and shapes the coupling/decoupling of riverine DBC and

452 DOC. DBC leaching experiments with charcoal as well as soils affected by atmospheric

453 deposition of soot may clarify specific mechanisms of DBC leaching from various types of

454 BC in soils.

455

456 **5. Conclusions**

457 This study investigated the quantitative and qualitative relationships among DBC and DOC

458 in streams in a transitional area from a cool-temperate zone to a boreal zone in which

459 catchments were not affected by landscape fire for at least 110 years. The relatively low

460 polycondensation degree of DBC found in this study implies that atmospherically deposited

461 soot on the soil in the catchment, which can preferentially release poorly polycondensed

462 DBC, is an important source of riverine DBC and is one of the important processes in the

463 global BC cycle. A strong linear relationship was found between the DOC and DBC

464 concentrations, irrespective of the differences in watershed characteristics and seasons.

465 Furthermore, qualitative relationships were evident between DBC and bulk DOM. These

466 quantitative and qualitative relationships suggest that for landscapes with dominant inputs

467 of soot-derived BC, the transfer mechanisms of natural DOC and DBC are closely linked,

468 while this linkage for wildfire charcoal-derived DBC has been shown to be more complex.

469

470 **Acknowledgments**

476

477

478   **Author contributions**

479   Y.Y. contributed to the design of the research. Y.Y., N.Y., and H.S. conducted field

480   observations and water sampling. D.K. and N.Y. performed experiments in the laboratory.

481   Y.Y., D.K., and N.Y. analyzed the results. Y.Y. prepared the manuscript with inputs from

482   H.S.

483

484

485 **References**

486 Abiven, S., Hengartner, P., Schneider, M.P.W., Singh, N., Schmidt, M.W.I., 2011.

487 Pyrogenic carbon soluble fraction is larger and more aromatic in aged charcoal than in

488 fresh charcoal. Soil Biol. Biochem. 43, 1615-1617.

489 Aiken, G.R., McKnight, D.M., Wershaw, R.L., MacCarthy, P., 1985. Humic substances in

490 soil, sediment and water: Geochemistry, isolation and characterization. John Wiley &

491 Sons, New York.

492 Bao, H., Niggemann, J., Huang, D., Dittmar, T., Kao, S.- J., 2019. Different responses of

493 dissolved black carbon and dissolved lignin to seasonal hydrological changes and an

494 extreme rain event. J. Geophys. Res. 124, 479-493.

495 Bond, T.C., Doherty, S.J., Fahey, D.W., Forster, P.M., Berntsen, T., DeAngelo, B.J.,

496 Flanner, M.G., Ghan, S., Kärcher, B., Koch, D., Kinne, S., Kondo, Y., Quinn, P.K.,

497 Sarofim, M.C., Schultz, M.G., Schulz, M., Venkataraman, C., Zhang, H., Zhang, S.,

498 Bellouin, N., Guttikunda, S.K., Hopke, P.K., Jacobson, M.Z., Kaiser, J.W., Klimont,

499 Z., Lohmann, U., Schwarz, J.P., Shindell, D., Storelvmo, T., Warren, S.G., Zender,

500 C.S., 2013. Bounding the role of black carbon in the climate system: A scientific

501 assessment. J. Geophys. Res. 118, 5380-5552.

502 Bostick, K.W., Zimmerman, A.R., Wozniak, A.S., Mitra, S, Hatcher, P.G., 2018.

503 Production and composition of pyrogenic dissolved organic matter from a logical

504 series of laboratory-generated chars. Front. Earth Sci. 6, 43.

505 Chang, Z., Tian, L., Li, F., Zhou, Y., Wu, M., Steinberg, C.E.W., Dong, X., Pan, B., Xing,

506 B., 2018. Benzene polycarboxylic acid — A useful marker for condensed organic

507 matter, but not for only pyrogenic black carbon. Sci. Total Environ. 626, 660–667.

508   Coble, P.G., 2007. Marine optical biogeochemistry: The chemistry of ocean color. Chem.

509   Rev. 07, 402-418.

510   Coppola, A.I., Wiedemeier, D.B., Galy, V., Haghipour, N., Hanke, U.M., Nascimento,

511   G.S., Usman, M., Blattmann, T.M., Reisser, M., Freymond, C.V., Zhao, M., Voss, B.,

512   Wacker, L., Schefuß, E., Peucker-Ehrenbrink, B., Abiven, S., Schmidt, M.W.I.,

513   Eglinton, T.I., 2018. Global-scale evidence for the refractory nature of riverine black

514   carbon. Nat. Geosci. 11, 584-588.

515   Coppola, A.I., Seidel, M., Ward, N.D., Viviroli, D., Nascimento, G.S., Haghipour, N.,

516   Revels, B.N., Abiven, S., Jones, M.W., Richey, J.E., Eglinton, T.I., Dittmar, T.,

517   Schmidt, M.W.I., 2019. Marked isotopic variability within and between the Amazon

518   River and marine dissolved black carbon pools. Nat. Comm. 10, 4018.

519   Cotrufo, M.F., Boot, C.M., Kampf, S., Nelson, P.A., Brogan, D.J., Covino, T., Haddix,

520   M.L., MacDonald, L.H., Rathburn, S., Ryan-Bukett, S., Schmeer, S., Hall, E., 2016.

521   Redistribution of pyrogenic carbon from hillslopes to stream corridors following a

522   large montane wildfire. Glob. Biogeochem. Cycle 30, 1348–1355.

523   Cory, R.M., McKnight, D.M., 2005. Fluorescence spectroscopy reveals ubiquitous

524   presence of oxidized and reduced quinones in dissolved organic matter. Environ. Sci.

525   Technol. 39, 8142-8149.

526   Ding, Y., Yamashita, Y., Dodds, W.K., Jaffé, R., 2013. Dissolved black carbon in grassland

527   streams: Is there an effect of recent fire history? Chemosphere 90, 2557-2562.

528   Ding, Y., Cawley, K.M., da Cunha, C.N., Jaffé, R., 2014. Environmental dynamics of

529   dissolved black carbon in wetlands. Biogeochemistry 119, 259–273.

530   Ding, Y., Yamashita, Y., Jones, J., Jaffé, R., 2015. Dissolved black carbon in boreal forest

531   and glacial rivers of central Alaska: assessment of biomass burning versus

532   anthropogenic sources. Biogeochemistry 123, 15-25.

533   Dittmar, T., 2008. The molecular level determination of black carbon in marine dissolved

534   organic matter. Org. Geochem. 39, 396-407.

535   Dittmar, T., Koch, B., Hertkorn, N., Kattner, G., 2008. A simple and efficient method for

536   the solid-phase extraction of dissolved organic matter (SPE-DOM) from seawater.

537   Limnol. Oceanogr.: Methods 6, 230–235.

538   Dittmar, T., de Rezende, C.E., Manecki, M., Niggemann, J., Ovalle, A.R.C., Stubbins, A.,

539   Bernardes, M.C., 2012. Continuous flux of dissolved black carbon from a vanished

540   tropical forest biome. Nat. Geosci. 5, 618–622.

541   Güereña, D.T., Lehmann, J., Walter, T., Enders, A., Neufeldt, H., Odiwour, H., Biwott, H.,

542   Recha, J., Shepherd, K., Barrios, E., Wurster, C., 2015. Terrestrial pyrogenic carbon

543   export to fluvial ecosystems: Lessons learned from the White Nile watershed of East

544   Africa, Glob. Biogeochem Cycle 29, 1911–1928.

545   Hansen, H.P., Koroleff, F., 1999. Determination of nutrients, in: Grasshoff, K., Kremling,

546   K., Ehrhardt, M. (Eds.), Methods of Seawater Analysis. WILEY-VCH, Weinheim, pp.

547   159–228.

548   Hedges, J.I., Eglinton, G., Hatcher, P.G., Kirchman, D.L., Arnosti, C., Derenne, S.,

549   Evershed, R.P., Kögel-Knabner, I., de Leeuw, J.W., Littke, R., Michaelis, W.,

550   Rullkötter, J., 2000. The molecularly-uncharacterized component of nonliving organic

551   matter in natural environments. Org. Geochem. 31, 945-958.

552 Helms, J.R., Stubbins, A., Ritchie, J.D., Minor, E.C., Kieber, D.J., Mopper, K., 2008.

553   Absorption spectral slopes and slope ratios as indicators of molecular weight, source,

554   and photobleaching of chromophoric dissolved organic matter. Limnol. Oceanogr. 53,

555   955-969.

556 Hino, S., Satoh, D., Okamura, A., Kikuchi, S., Ishikawa, Y., Mikami, H., Igarashi, S.,

557   Takano, K., 2006. Characters of nutrient load from influent rivers of Lake Shumarinai.

558   IDEA project Interrim Report 39-42.

559 Hockaday, W.C., Grannas, A.M., Kim, S., Hatcher, P.G., 2006. Direct molecular evidence

560   for the degradation and mobility of black carbon in soils from ultrahigh-resolution

561   mass spectral analysis of dissolved organic matter from a fire-impacted forest soil.

562   Org. Geochem. 37, 501-510.

563 Hockaday, W.C., Grannas, A.M., Kim, S., Hatcher, P.G., 2007. The transformation and

564   mobility of charcoal in a fire-impacted watershed. Geochim. Cosmochim. Acta 71,

565   3432-3445.

566 Holmes, R.M., McClelland, J.W., Raymond, P.A., Frazer, B.B., Peterson, B.J., Stieglitz,

567   M., 2008. Lability of DOC transported by Alaskan rivers to the Arctic Ocean.

568   Geophys. Res. Lett., 35, L03402.

569 Inamdar, S., Rupp, J., Mitchell, M., 2008. Differences in dissolved organic carbon and

570   nitrogen responses to storm-event and ground-water conditions in a forested, glaciated

571   watershed in western New York. J. Am. Water Resour. Assoc. 44, 1458-1473.

572 Jaffé, R., Ding, Y., Niggemann, J., Vähätalo, A.V., Stubbins, A., Spencer, R.G.M.,

573   Campbell, J., Dittmar, T., 2013. Global charcoal mobilization from soils via

574   dissolution and riverine transport to the oceans. Science 340, 345-347.

575 Jones, M.W., Quine, T.A., de Rezende, C.E., Dittmar, T., Johnson, B., Manecki, M.,

576   Marques, J.S.J., de Aragão, L.E.O.C., 2017. Do regional aerosols contribute to the

577   riverine export of dissolved black carbon? J. Geophys. Res. 122, 2925–2938.

578 Jones, M.W., Santín, C., van der Werf, G.R., Doerr, S.H., 2019a. Global fire emissions

579   buffered by the production of pyrogenic carbon. Nat. Geosci. 12, 742-747.

580 Jones, M.W., de Aragão, L.E.O.C., Dittmar, T., de Rezende, C.E., Almeida, M.G., Johnson,

581   B.T., Niggemann, J., Rangel, T.P., Quine, T.A., 2019b. Environmental controls on the

582   riverine export of dissolved black carbon. Glob. Biogeochem. Cycle 33, 849–874.

583 Jones, M.W., Coppola, A.I., Santín, C., Dittmar, T., Jaffé, R., Doerr, S.H., Quine, T.A.,

584   2020. Fires prime terrestrial organic carbon for riverine export to the global oceans.

585   Nat. Comm. 11, 2791.

586 Kappenberg, A., Bläsing, M., Lehndorff, E., Amelung, W., 2016. Black carbon assessment

587   using benzene polycarboxylic acids: Limitations for organic-rich matrices.

588   Org. Geochem. 94, 47-51.

589 Knicker, H., 2011. Pyrogenic organic matter in soil: Its origin and occurrence, its chemistry

590   and survival in soil environments. Quat. Int. 243, 251-263.

591 Kuhlbusch, T.A., 1998. Black carbon and the carbon cycle. Science 280, 1903-1904.

592 Kothawala, D.N., Roehm, C., Blodau, C., Moore, T.R., 2012. Selective adsorption of

593   dissolved organic matter to mineral soils. Geoderma 189–190, 334–342.

594 Lawaetz, A.J., Stedmon, C.A., 2009. Fluorescence intensity calibration using Raman scatter

595   peak of water. Appl. Spectrosc. 63, 936–940.

596 Mari, X., Lefèvre, J., Torréton, J.P., Bettarel, Y., Pringault, O., Rochelle-Newall, E.,

597   Marchesiello, P., Menkes, C., Rodier, M., Migon, C., Motegi, C., Weinbauer, M.G.,

598   Legendre, L., 2014. Effects of soot deposition on particle dynamics and microbial

599   processes in marine surface waters, Global Biogeochem. Cycles 28, 662–678.

600   Mari ,X., Guinot, B., Thuoc, C.V., Brune, J., Lefebvre, J.-P., Angia Sriram, P.R.,

601   Raimbault. P., Dittmar, T., Niggemann, J., 2019. Biogeochemical impacts of a black

602   carbon wet deposition event in Halong Bay, Vietnam. Front. Mar. Sci. 6, 185.

603   Marques, J.S.J, Dittmar, T., Niggemann, J., Almeida, M.G., Gomez-Saez, G.V., Rezende,

604   C.E., 2017. Dissolved black carbon in the headwaters-to-ocean continuum of Paraíba

605   Do Sul River, Brazil. Front. Earth Sci. 5, 11.

606   Masiello, C.A., 2004. New directions in black carbon organic geochemistry. Mar. Chem.

607   92, 201-213.

608   Masiello, C.A., Druffel, E.R.M., 1998. Black carbon in deep-sea sediments. Science 280,

609   1911-1913.

610   McKnight, D.M., Harnish, R., Wershaw, R.L., Baron, J.S., Schiff, S., 1997. Chemical

611   characteristics of particulate, colloidal, and dissolved organic material in Loch Vale

612   Watershed, Rocky Mountain National Park. Biogeochemistry 36, 99-124.

613   McKnight, D.M., Boyer, E.W., Westerhoff, P.K., Doran, P.T., Kulbe, T., Andersen, D.T.,

614   2001. Spectrofluorometric characterization of dissolved organic matter for indication

615   of precursor organic material and aromaticity. Limnol. Oceanogr. 46, 38–48.

616   Murphy, K.R., Butler, K.D., Spencer, R.G.M., Stedmon, C.A., Boehme, J.R., Aiken, G.R.,

617   2010. Measurement of dissolved organic matter fluorescence in aquatic environments:

618   An interlaboratory comparison. Environ. Sci. Technol. 2010, 9405–9412.

619 Myers-Pigg, A.N., Louchouarn, P., Amon, R.M.W., Prokushkin, A., Pierce, K., Rubtsov,

620   A., 2015. Labile pyrogenic dissolved organic carbon in major Siberian Arctic rivers:

621   Implications for wildfire-stream metabolic linkages. Geophys. Res. Lett. 42, 377–385.

622 Nakane, M., Ajioka, T., Yamashita, Y., 2017. Distribution and sources of dissolved black

623   carbon in surface waters of the Chukchi Sea, Bering Sea, and the North Pacific Ocean.

624   Front. Earth Sci. 5, 34.

625 Ogawa, A., Shibata, H., Suzuki, K., Mitchell, M.J., Ikegami, Y., 2006. Relationship of

626   topography to surface water chemistry with particular focus on nitrogen and organic

627   carbon solutes within a forested watershed in Hokkaido, Japan. Hydrol. Process. 20,

628   251–265.

629 Ozawa, M., Shibata, H., Satoh, F., Sasa, K., 2001. Effects of surface soil removal on

630   dynamics of dissolved inorganic nitrogen in a snow-dominated forest. Sci. World. 1,

631   527-533.

632 Oswald, C.J., Branfireun, B.A., 2014. Antecedent moisture conditions control mercury and

633   dissolved organic carbon concentration dynamics in a boreal headwater catchment.

634   Water Resour. Res. 50, 6610–6627.

635 Roebuck, J.A., Seidel, M., Dittmar, T., Jaffé, R., 2018a. Land use controls on the spatial

636   variability of dissolved black carbon in a subtropical watershed. Environ. Sci.

637   Technol. 52, 8104−8114.

638 Roebuck, J.A., Medeiros, P.M., Letourneau, M.L., Jaffé, R., 2018b. Hydrological controls

639   on the seasonal variability of dissolved and particulate black carbon in the Altamaha

640   River, GA. J. Geophys. Res. 123, 3055–3071.

641   Santín, C., Doerr, S.H., Kane, E.S., Masiello, C.A., Ohlson, M., de la Rosa J.M., Preston

642   C.M., Dittmar, T., 2016. Towards a global assessment of pyrogenic carbon from

643   vegetation fires. Glob. Chang. Biol. 22, 76-91.

644   Santos, F., Wagner, S., Rothstein, D., Jaffé, R., Miesel, J.R., 2017. Impact of a historical

645   fire event on pyrogenic carbon stocks and dissolved pyrogenic carbon in spodosols in

646   northern Michigan. Front. Earth Sci. 5, 80.

647   Seki, O., Nakatsuka, T., Shibata, H., Kawamura, K., 2010. A compound-specific *n*-alkane

648          $\delta^{13}C$ and δD approach for assessing source and delivery processes of terrestrial

649   organic matter within a forested watershed in northern Japan. Geochim. Cosmochim.

650   Acta 74, 599-613.

651   Stubbins, A., Hood, E., Raymond, P.A., Aiken, G.R., Sleighter, R.L., Hernes, P.J., Butman,

652   D., Hatcher, P.G., Striegl, R.G., Schuster, P., Abdulla, H.A.N., Vermilyea, A.W.,

653   Scott, D.T., Spencer, R.G.M., 2012. Anthropogenic aerosols as a source of ancient

654   dissolved organic matter in glaciers. Nat. Geosci., 5, 198-201.

655   Stubbins, A., Spencer, R.G.M., Mann, P.J., Holmes, R.M., McClelland, J.W., Niggemann,

656   J., Dittmar, T., 2015. Utilizing colored dissolved organic matter to derive dissolved

657   black carbon export by arctic rivers. Front. Earth Sci. 3, 63.

658   Stubbins, A., Silva, L.M., Dittmar, T., Van Stan, J.T., 2017. Molecular and optical

659   properties of tree-derived dissolved organic matter in throughfall and stemflow from

660   live oak and eastern red cedar. Front. Earth Sci. 5, 22.

661   Tanaka, K., Kuma, K., Hamasaki, K., Yamashita, Y., 2014. Accumulation of humic-like

662   fluorescent dissolved organic matter in the Japan Sea. Sci. Rep. 4, 5292.

663   Wang, X., Xu, C., Druffel, E.M., Xue, Y., Qi., 2016. Two black carbon pools transported

664   by the Changjiang and Huanghe Rivers in China, Glob. Biogeochem. Cycle 30, 1778-

665   1790.

666   Wagner, S., Cawley, K.M., Rosario-Ortiz, F.L., Jaffé, R., 2015. In-stream sources and links

667   between particulate and dissolved black carbon following a wildfire. Biogeochemistry

668   124, 145-161.

669   Waggoner, D.C., Chen, H., Willoughby, A.S., Hatcher, P.G., 2015. Formation of black

670   carbon-like and alicyclic aliphatic compounds by hydroxyl radical initiated

671   degradation of lignin. Org. Geochem. 82, 69-76.

672   Wagner, S., Ding, Y., Jaffé, R., 2017. A new perspective on the apparent solubility of

673   dissolved black carbon. Front. Earth Sci. 5, 75.

674   Wagner, S., Jaffé, R., Stubbins, A., 2018. Dissolved black carbon in aquatic ecosystems.

675   Limno. Oceanogr. Lett. 3, 168-185.

676   Wagner, S., Brandes, J., Spencer, R.G.M., Ma, K., Rosengard, S.Z., Moura, J,M.S.,

677   Stubbins, A., 2019a. Isotopic composition of oceanic dissolved black carbon reveals

678   non-riverine source. Nat. Comm., 10, 5064.

679   Wagner, S., Brantley, S., Stuber, S., Van Stan, J.V., Whitetree, A., Stubbins, A., 2019b.

680   Dissolved black carbon in throughfall and stemflow in a fire-managed longleaf pine

681   woodland. Biogeochemistry 146, 191-207.

682   Weishaar, J.L., Aiken, G.R., Bergamaschi, B.A., Fram, M.S., Fujii, R., Mopper, K., 2003.

683   Evaluation of specific ultraviolet absorbance as an indicator of the chemical

684   composition and reactivity of dissolved organic carbon. Environ. Sci. Technol. 37,

685   4702-4708.

686 Wilson, H.F., Saiers, J.E., Raymond, P.A., Sobczak, W.V., 2013. Hydrologic drivers and

687   seasonality of dissolved organic carbon concentration, nitrogen content,

688   bioavailability, and export in a forested New England stream. Ecosystems 16, 604–

689   616.

690 Wozniak, A.S., Goranov, A.I., Mitra, S., Bostick, K.W., Zimmerman, A.R., Schlesinger,

691   D.R., Myneni, S., Hatcher, P.G., 2020. Molecular heterogeneity in pyrogenic

692   dissolved organic matter from a thermal series of oak and grass chars. Org. Geochem.

693   148, 104065.

694 Zhu, C., Kanaya, Y., Yoshikawa-Inoue, H., Irino, T., Seki, O., Tohjima, Y., 2019. Sources

695   of atmospheric black carbon and related carbonaceous components at Rishiri Island,

696   Japan: The roles of Siberian wildfires and of crop residue burning in China. Environ.
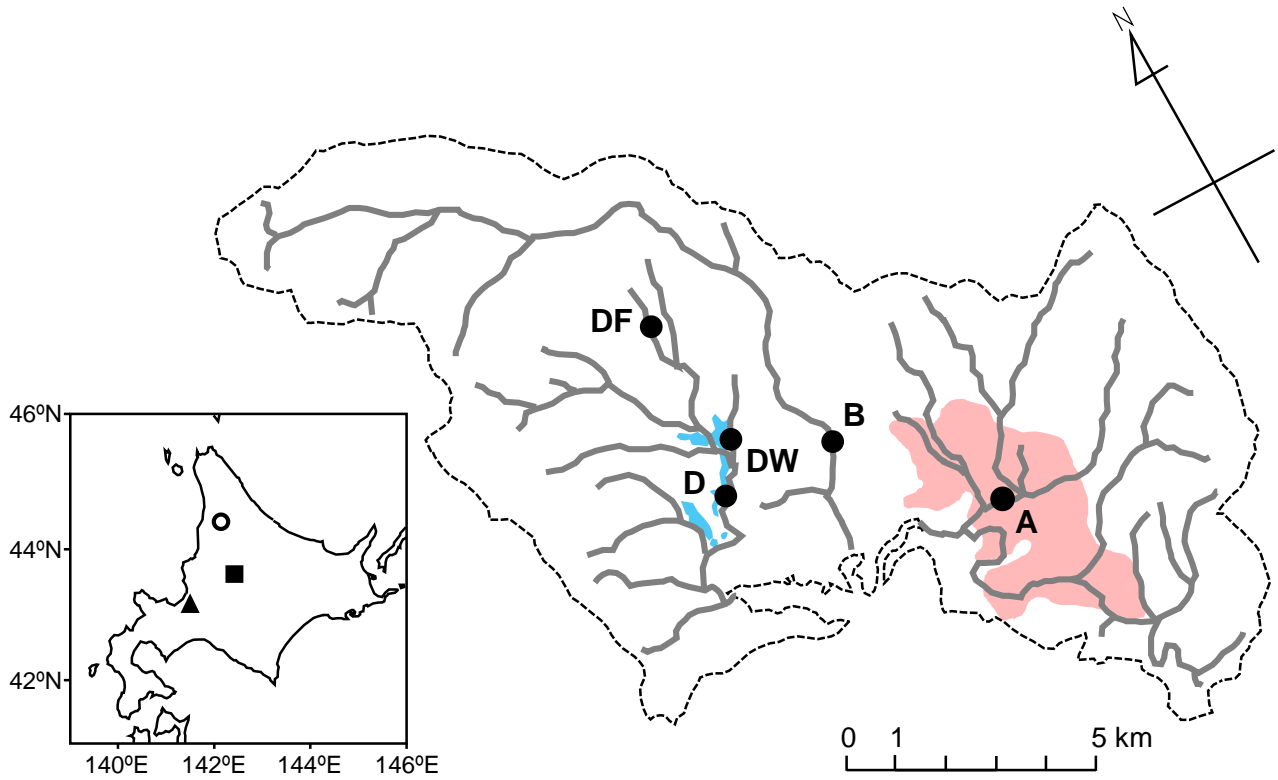
697   Pollut. 247, 55-63.

698

699

Figure 1. Map of the sampling sites and their watersheds. Blue and red shadows in watersheds indicate wetlands and pastureland, respectively. Open circle, closed triangle, and closed square represent Hokkaido University's Uryu Experimental Forest (UREF), Sapporo, and Asahikawa, respectively. D, B, and A represent sampling sites of the Dorokawa River, Butokamabetsu River, and Akaishi River, respectively. DF and DW represent sampling sites of tributaries of the Dorokawa River, whose watersheds were covered by forest and wetlands, respectively.
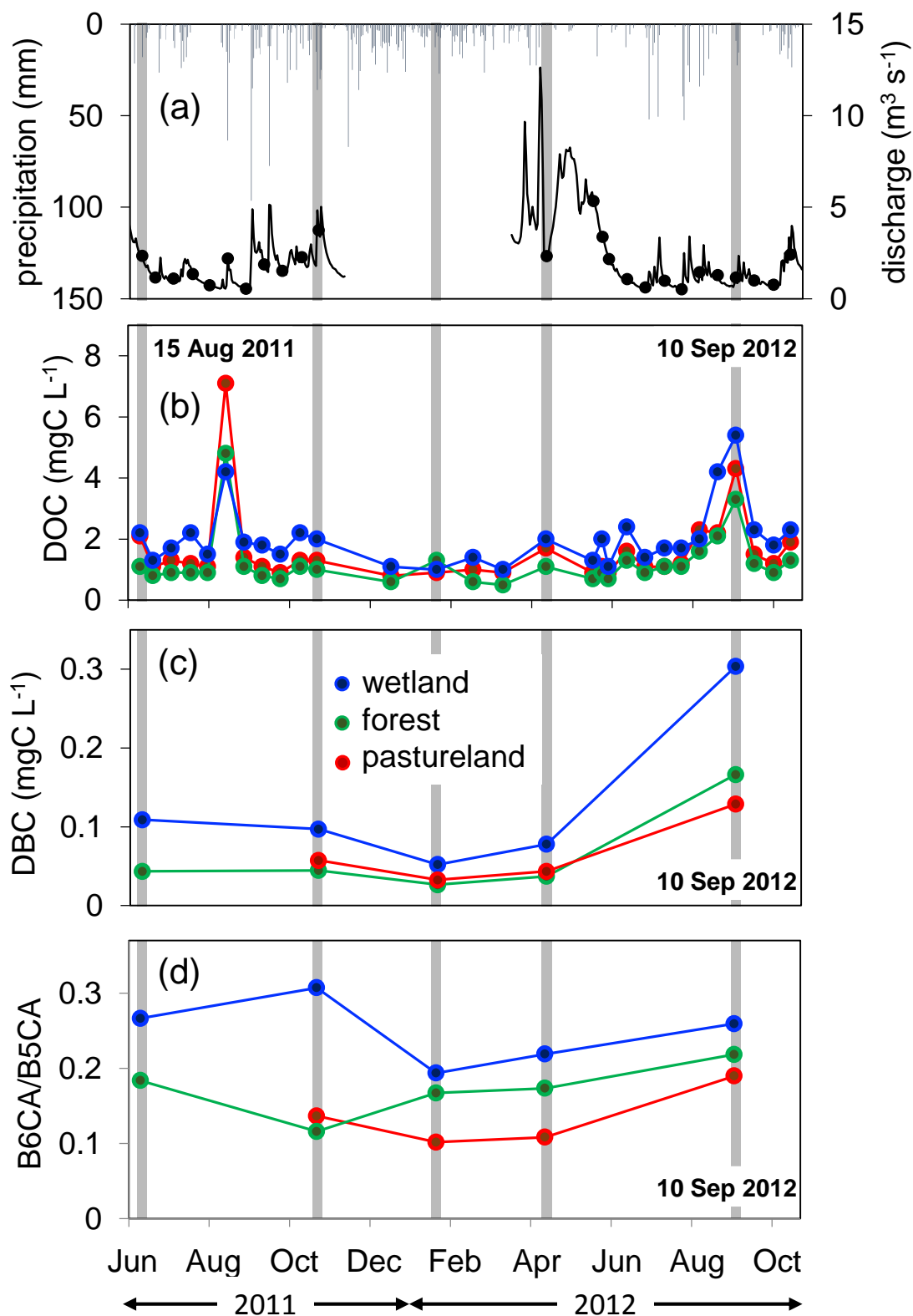
Figure 2. Temporal variations in precipitation (a); stream discharge at the Butokamabetsu River site (B) (a); DOC concentration at the Dorokawa River (D), B, and Akaishi River sites (A) (b); DBC concentration at sites D, B, and A (c); and B6CA/B5CA at sites D, B, and A (d). Black closed circles on stream discharge (a) and gray hatches in all panels (a–d) indicate sampling days of DOC and DBC, respectively. Blue, green, and red symbols indicate D (wetland), B (forest), and A (pastureland) sites, respectively.
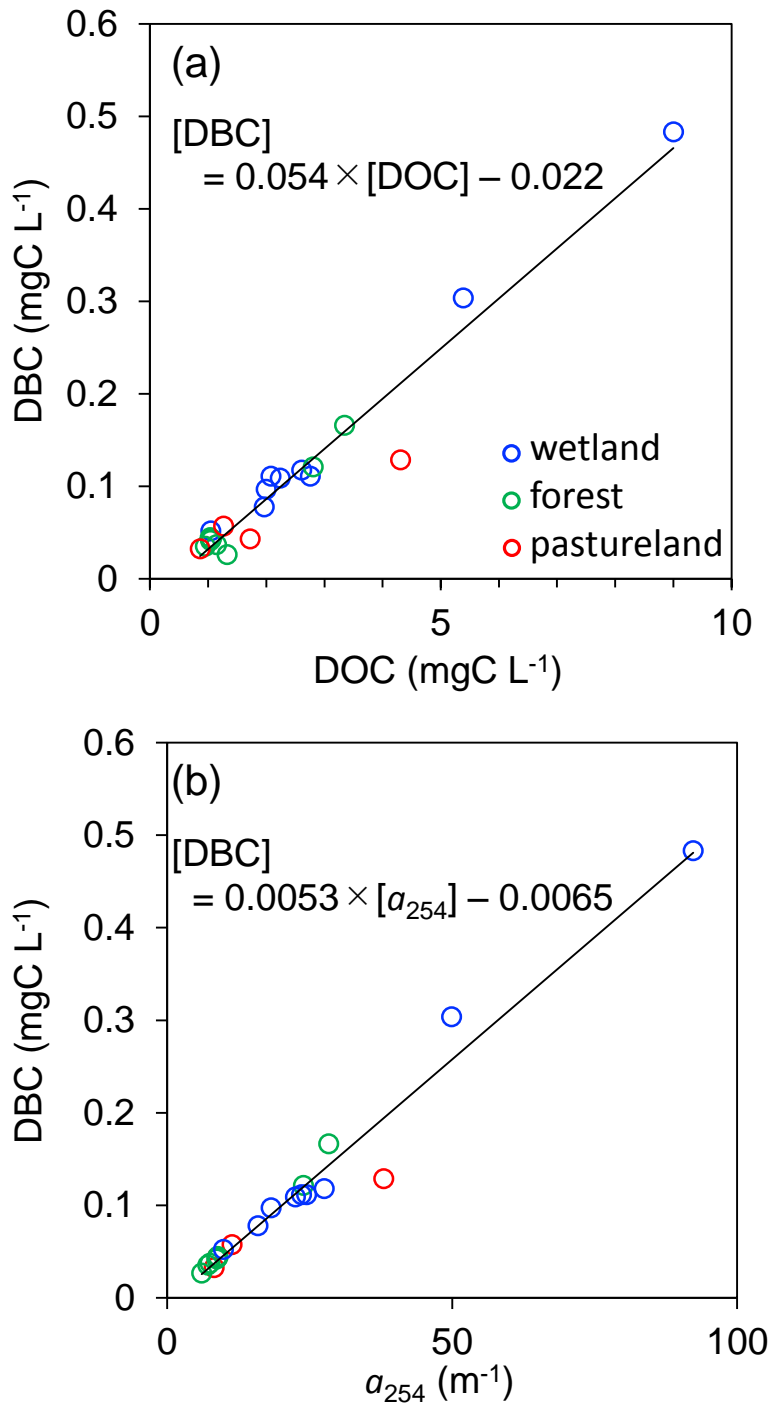
Figure 3. Relationships between DBC concentration and DOC concentration (a) and a_{254} (b) for all samples collected from all sites. For the DBC–DOC regression (a), standard error of the slope = 0.003; standard error of the intercept = 0.009; $r^2 = 0.95$; $n = 21$; $p < 0.01$. For the DBC–a_{254} regression (b), standard error of the slope = 0.0002; standard error of the intercept = 0.0066; $r^2 = 0.97$; $n = 21$; $p < 0.01$. Blue, green, and red symbols indicate the wetland area (Dorokawa River and wetland tributary of Dorokawa River), forest area (Butokamabetsu River and forested tributary of Dorokawa River), and pastureland area (Akaishi River), respectively.
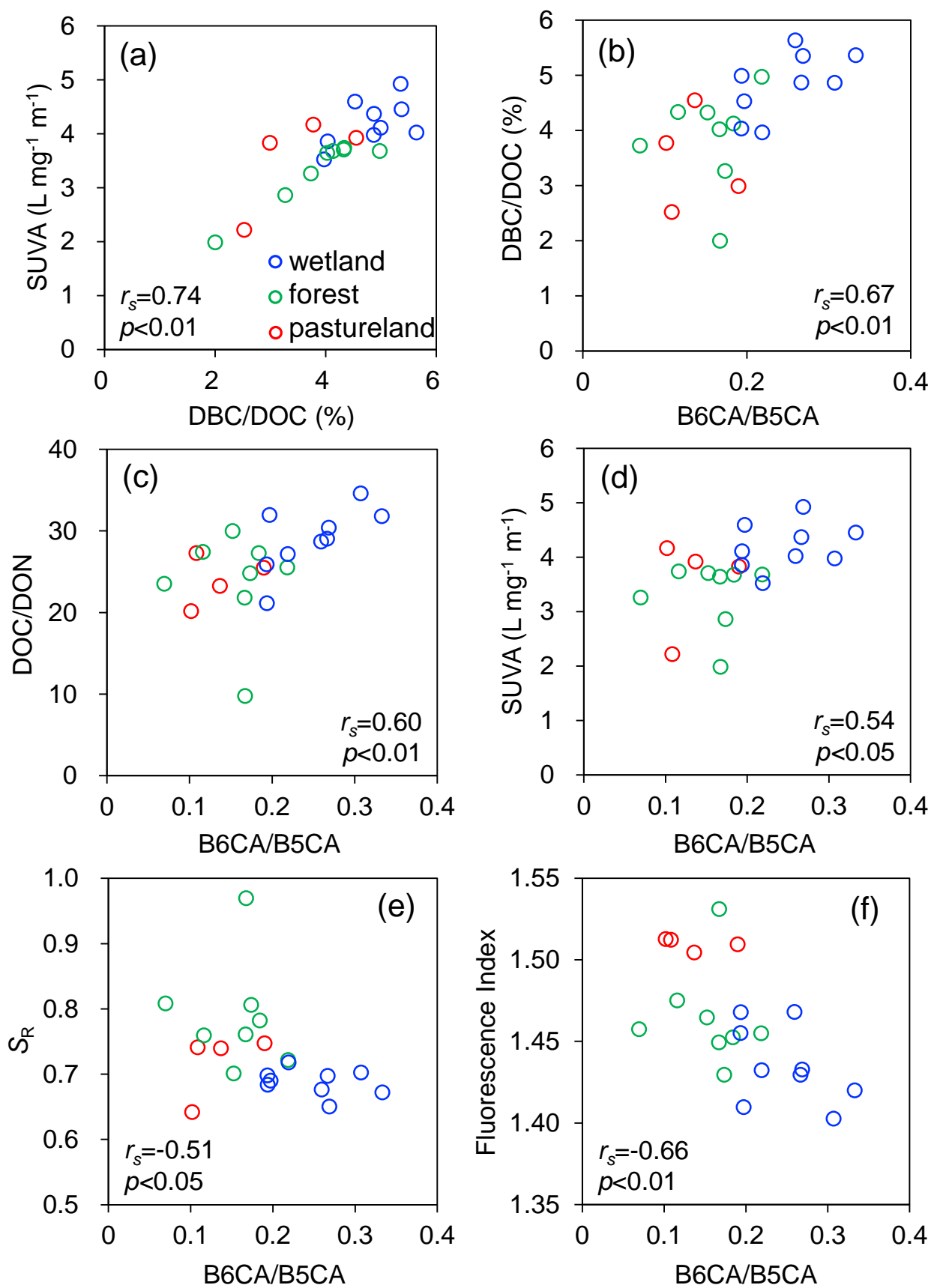
Figure 4. Relationships among qualitative parameters of DBC and bulk DOM. SUVA *vs.* DBC/DOC (a), DBC/DOC *vs.* B6CA/B5CA (b), DOC/DON *vs.* B6CA/B5CA (c), SUVA *vs.* B6CA/B5CA (d), S_R *vs.* B6CA/B5CA (e), and fluorescence index *vs.* B6CA/B5CA (f). *r* and *p* values are the results of Spearman's rank correlation test. A confidence level (α) of 95% was used. Blue, green, and red symbols indicate the wetland area (Dorokawa River and wetland tributary of Dorokawa River), forest area (Butokamabetsu River and forested tributary of Dorokawa River), and pastureland area (Akaishi River), respectively.